

THE ROLE OF CAVEOLAE IN THE LOSS OF ERK2 ACTIVATION IN  
STRETCHED SKELETAL MYOTUBES

A Dissertation  
Presented to  
The Academic Faculty

By

Anne Claire Bellott

In Partial Fulfillment  
Of the Requirements for the Degree  
Master of Science in the School of Mechanical Engineering, Bioengineering Program

Georgia Institute of Technology  
July 2004

# The Role of Caveolae in the Loss of ERK2 Activation in Stretched Skeletal Myotubes

Approved by:

Dr. Tom Burkholder, Advisor

Dr. Hanjoong Jo

Dr. Alfred Merrill

July 12, 2004

## ACKNOWLEDGEMENT

Many thanks go to my advisor, Dr. Tom Burkholder, for all the work he did to help me finish my thesis on time. Kishan Patel and Keith Van Antwerp also deserve my thanks for the work they did in lab to help me along the way. In addition, I wish to thank Dr. Alfred Merrill and Dr. Hanjoong Jo for agreeing to serve on my thesis committee. I truly appreciate all the work that everyone has done to get me here.

## TABLE OF CONTENTS

Acknowledgements	iii
List of Figures	vi
Summary	viii
Chapter 1 Introduction	9
1.1 Stretch	9
1.2 Mechanotransduction	12
1.3 Hypothesis	15
1.4 Experimental Design	16
Chapter 2 Methods and Materials	18
2.1 Isolation and Growth of Neonatal Mouse Myoblasts	18
2.2 TEM Pictures	20
2.3 Cell Maintenance and Membrane Seeding	20
2.4 Stretch Experiment Prep.	21
2.5 Stretch Experiments	23
2.6 Caveolin-3 Knockdown	24
2.7 Bicinchoninic Acid Protein Assay	26
2.8 Protein Analysis	26
2.9 Cell morphology	27
2.10 Immunostaining of Membranes for Caveolae	28
2.11 Statistical Analysis	28
Chapter 3 Results	29

3.1 Myogenic Testing	29
3.2 Fusion Index	29
3.3 Caveolae Morphology	30
3.4 Optimization of the Stretch Protocol	30
3.5 Treatment with Methyl-Beta-Cyclodextrin (M $\beta$ CD)	31
3.6 siRNA Knockdown	33
3.7 Stretch Experiments at 22°C	39
Chapter 4 Discussion	43
4.1 Clinical Importance	47
References	50

## LIST OF FIGURES

Figure 2.1	Stretcher Cassette	21
Figure 2.2	Cassette Stretcher	22
Figure 2.3	Image of aligned and fused myotubes grown on a well of a cassette	23
Figure 3.1	Desmin stained myoblasts in conventional (A) and phase-contrast (B) illumination	29
Figure 3.2	Caveolae-sized structures in unstretched cultures always displayed the classical flask-shaped morphology in <i>mdx</i> myotubes (A). Stretched myotubes also displayed putatively pit- or dome-shaped invaginations consistent with opening of caveolae in C57 myotubes (B).	30
Figure 3.3	Stretch induced ERK2 phosphorylation depends on both amplitude and velocity. (†= $p < 0.01$ for velocity, * = $p < 0.01$ for amplitude, Mean $\pm$ S.D.)	31
Figure 3.4	ERK2 phosphorylation in response to stretch following 1hr pre-incubation with M $\beta$ CD (*= $p < 0.01$ for pre-incubation media, Mean $\pm$ S.D.). (parenthetical numbers provide sample number)	32
Figure 3.5	Static cells treated with 0.1% M $\beta$ CD over time. (parenthetical numbers provide sample number)	33
Figure 3.6	Transfection with fluorescein-tagged RNA oligos © revealed efficient uptake of RNA. Untreated control (A) and light microscope matching “(C)” (B) for comparison.	34
Figure 3.7	Static transfection with all three siRNA results in knockdown of caveolin-3 (*= $p < 0.001$ , Mean $\pm$ S.D.). (parenthetical numbers provide sample number)	34
Figure 3.8	Immunostaining of a non-transfected (A) and a cav3-1 transfected (B) membrane. In (A) the ↓ refers to the highly localized and membrane-associated caveolin-3. In (B) the ↓ refers to the low fluorescein and distributed caveolin-3.	35
Figure 3.9	Alterations in ERK2 activation following siRNA knockdown with all 3 caveolin-3 siRNA's . (parenthetical numbers provide sample number)	36

Figure 3.10	Time course of Cav-3 knockdown ( $p < 0.0001$ for transfected wells vs. non-transfected, MEAN $\pm$ S.E.) (parenthetical numbers provide sample number)	37
Figure 3.11	Knockdown of caveolin-3 following transfection with cav3-1 in stretched and unstretched myotubes ( $*=p < 0.001$ for pre-incubation, Mean $\pm$ S.D.)(parenthetical numbers provide sample number).	38
Figure 3.12	Phosphorylated ERK2 compared in transfected vs. non-transfected cells ( $*=p < 0.05$ for pre-incubation, Mean $\pm$ S.D.)(parenthetical numbers provide sample number).	39
Figure 3.13	Caveolin-3 expression in 37°C and 22°C samples with and without previous transfection ( $*=p < 0.005$ for pre-incubation, MEAN $\pm$ S.D.)(parenthetical numbers provide sample number)	40
Figure 3.14	PhosphoERK activation in the 37°C vs. 22°C samples ( $*=p < 0.02$ , $\# = p < 0.002$ , $\dagger = p < 0.05$ by pre-incubation, MEAN $\pm$ S.D.)(parenthetical numbers provide sample number)	41
Figure 3.15	FGF stimulated ERK2 phosphorylation at room temperature (22°C),(parenthetical numbers provide sample number)	42

## SUMMARY

Skeletal muscle function is important to the human body for daily activities. Mechanical signals are critical to the maintenance of that function. Muscle diseases, such as the muscular dystrophies, in which the force transmission apparatus is compromised, have devastating effects on muscle function and quality of life. Mechanical signals activate intracellular signaling to maintain function. ERK2 has been shown to be quickly and strongly upregulated following stretch, leading to cell proliferation. Stretch has been shown to cause deformation of caveolae, invaginations of the plasma membrane that inhibit ERK signaling. This leads to the hypothesis that stretch induced deformation of caveolae may initiate mechanotransduction by activating ERK2. Reducing caveolin-3 expression via siRNA knockdown eradicated the stretch-induced effect on ERK2 activation, indicating that caveolin is required for the stretch response. Stabilizing caveolae structure by temperature reduction or destabilizing caveolae by cholesterol depletion resulted in changes consistent with the hypothesis that proper caveolae structure plays an important role in inhibition of signaling molecules and that deformation mediates mechanotransduction, resulting in changes in activation of ERK2.

# CHAPTER 1

## INTRODUCTION

### 1.1 Stretch

Skeletal muscle function is important to the human body for a variety of reasons. Day-to-day activities can be compromised by muscle atrophy secondary to sickness, obesity, or old age. There have been a variety of ways that previous work has attempted to illustrate the importance of stretch. Among these is muscle growth resulting from post-natal passive stretch, atrophy due to old age or sickness, and illnesses such as muscular dystrophy. For example, aging, a major cause of muscle loss, is associated with a decrease in overall muscle mass due to loss of muscle fibers, as well as, reduction in fiber size (Lexell, *et al.* 1988).

Stretch-created mechanical signals are critical to the maintenance of muscle mass and function (Carson and Wei, 2000; Aronson, *et al.* 1997; Goldspink, Williams, and Simpson, 2002). Mechanical signals lead to activation of signaling cascades, satellite cell proliferation, and cell differentiation, but the mechanism by which cells initiate mechanotransduction remains unclear (Carson and Wei, 2000; Tatsumi, *et al.* 2001; Powell, *et al.* 2002; Goldspink, Williams, and Simpson, 2002; Sadoshima and Izumo, 1997). Understanding how stretch mediates biochemical signaling is of great importance not only to fighting muscular dystrophy but also to help the elderly and sick maintain an independent and healthy life-style. Caveolae have been shown to unfold during stretch and associate with a variety of inactive signaling molecules (Dulhunty & Franzini-

Armstrong, 1975; Li, *et al.* 1996, Rybin *et al.* 1999, Galbiati, *et al.* 2000). Caveolae may be a model for mechanotransduction in muscle cells.

### *1.1.1 Postnatal Growth and Exercise*

Mechanical signals, such as post-natal growth and exercise, are critical to the normal development and maintenance of muscle (Carson and Wei, 2000; Aronson, *et al.* 1997; Goldspink, Williams, and Simpson, 2002). Passive stretch resulting from bone elongation is one of the critical determinants of postnatal muscle growth (Williams and Goldspink, 1976). Stretch-induced mechanical stimulation of muscles has been linked to gene activation, increased protein synthesis, satellite cell proliferation, and differentiation (Powell, *et al.* 2002; Goldspink, Williams & Simpson, 2002; Tatsumi, *et al.* 2001; Sadoshima & Izumo, 1997). Passive stretch also increases the presence of various growth factors, including insulin-like growth factor 1 (IGF-1) (Loughna, Mason and Bates, 1992).

Exercise is largely emphasized these days as an important way to remain healthy and maintain muscle mass. Exercise has been shown to increase protein synthesis and gene expression (Goldberg, 1968; Chen, *et al.* 2002). It can also initiate activation or augmentation of other molecules such as growth factors. During chronic stretch, IGF-1 is released (McKoy, *et al.* 1999) and stimulates protein synthesis and satellite cell proliferation and differentiation (Florini, *et al.* 1996).

### 1.1.2 Disruptions in mechanical signaling

Reductions in mechanical stimuli, or disruption of the mechanotransduction machinery, leads to a corresponding loss of muscle function. As people age, they tend to develop a more sedentary lifestyle, and this reduction of mechanical signaling leads to atrophy in skeletal muscles (Lexell, *et al.* 1988). Disuse can lead to a decrease in the activation levels of signaling cascades such as ERK2 (Williamson, *et al.* 2003) and a decrease in muscle size and fiber size and number (Lexell, *et al.* 1988).

Illness can also lead to a disruption of normal levels of muscle activation. Muscular dystrophies are a family of genetic diseases, which result in the disruption of the normal muscle growth and function (Galbiati, *et al.* 2000). Duchenne muscular dystrophy (DMD) is the most common form of muscular dystrophy and is caused by a lack of dystrophin in the muscle cells (Hoffman, *et al.* 1987). DMD is characterized by a loss of dystrophin and the presence of regenerating or immature muscle fibers (Galbiati, *et al.* 2000). *Mdx* mice, the animal model for DMD, and DMD humans both show a compensatory increase in caveolin-3 expression in their muscles and increased density of caveolae (Vaghy, *et al.* 1998; Repetto, *et al.* 1999).

Limb-girdle muscular dystrophy 1C (LGMD-1C) is a mild form of muscular dystrophy that is caused by a mutation in caveolin-3, which causes caveolin-3 to be targeted for degradation (Galbiati, *et al.* 2000). The mutant caveolin-3 is sequestered at the Golgi apparatus followed by proteasomal degradation and reduction by roughly 95% (Galbiati, *et al.* 2000; Minetti, *et al.* 2002). Similar to LGMD-1C, targeted disruption of caveolin-3 leads to a decrease in caveolae at the sarcolemma, malformation of the T-

tubule system, myopathic changes, and a loss of the dystrophin-glycoprotein complex from lipid rafts (Galbiati, *et al.* 2000). This demonstrates that proper caveolae function is important to the normal growth and development of skeletal muscle.

## 1.2 Mechanotransduction

Mechanotransduction is the transfer of an external mechanical signal at the cell surface into an internal signal. Mechanical signaling can trigger events ranging from increased gene expression and protein synthesis to cell differentiation and proliferation (Goldberg, 1968; Chen, *et al.* 2002; Powell, *et al.* 2002; Goldspink, Williams & Simpson, 2002; Tatsumi, *et al.* 2001; Sadoshima & Izumo, 1997). Several mechanisms, including integrins (Maniotis, *et al.* 1997; Carson and Wei, 2000), membrane disruption (McNeil, *et al.* 1997; Lin, *et al.* 1997), and caveolae (Li, *et al.* 1996), have been implicated in mechanotransduction.

### 1.2.1 Integrins

Integrins are a large family of transmembrane glycoprotein complexes mediating cell adhesion (Mayer, 2003). Integrins have been shown to play a role in myoblast migration from the somite as well as in terminal differentiation into myotubes in developing muscle (Mayer, 2003). Maniotis and colleagues (1997), using ECM coated beads to supply loads directly to integrins on skeletal muscle cells, found that deformation of the cell membrane resulted in nuclear deformation. This suggests that

tension passed directly through the cytoskeleton to the nucleus may directly deform nuclear pores to alter gene transcription. Integrins have also been shown to activate FAK, PI3-K, PKC, Ras, and Rho (Carson and Wei, 2000). It is, however, difficult to separate the ligand-binding role of integrins from their mechanical role, and the mechanism by which integrins might mediate mechanotransduction remains unclear.

### *1.2.2 Membrane Disruption*

Skeletal muscles undergo one of the highest rates of membrane disruption found in animal muscles, which may lead to the release of cytosolic growth factors and calcium influx (McNeil and Steinhardt, 1997). Following disruption, bFGF, a potent stimulator of cell proliferation, and aFGF are released in cell culture (McNeil, *et al.* 1989). The movement of growth factors and calcium following stretch strongly suggest that membrane disruption plays at least a partial role in inducing signaling cascades in muscle cells (McNeil and Steinhardt, 1997). Membrane disruption is a dramatic and potentially lethal event, and the membrane of mechanically active cells maintain a reserve of membrane material in caveolae to minimize the incidence of membrane disruption (Dulhunty & Franzini-Armstrong, 1975)

### *1.2.3 Caveolae*

Caveolae are rounded, smooth invaginations of the plasma membrane 50-100nm in diameter (Galbiati, *et al.* 2000). Caveolae are enriched in sphingolipids and

cholesterol, and their structure depends on the structural protein, caveolin (Rothberg, *et al.* 1992; Schlegel, *et al.* 1998). Caveolae have been shown to unfold during stretch as a means by which the cells shield themselves from damage (Dulhunty & Franzini-Armstrong, 1975). Many signaling molecules, including MEK, Src, and PKC $\alpha$ , have also been shown to localize at caveolae (Li, *et al.* 1996; Rybin, *et al.* 1999).

Caveolae are a subset of lipid rafts, microdomains within the plasma membrane that have a high concentration of sphingolipids and cholesterol (Li, *et al.* 1996; Rybin, *et al.* 1999; Veiga, *et al.* 2001). Veiga and colleagues (2001) showed that lipid rafts are temperature-dependent. At physiological temperatures, pure, synthetic sphingolipids exist in a gel phase having a melting temperature of  $\sim 42^{\circ}\text{C}$ . The addition of cholesterol allows for the sphingolipids to exist in a liquid-ordered state below their melting temperature, instead of in a gel state. The physical phase of the raft domains is strongly temperature dependent near  $37^{\circ}\text{C}$ . Of note, a shift to the gel phase occurs around  $20\text{-}30^{\circ}\text{C}$ , depending on the molar fraction of cholesterol (Veiga, *et al.* 2001). This phenomenon has long been used to block retrograde transport (Le and Nabi, 2003), and gelling the caveolae may prevent the mechanical deformation.

There are three known forms of the mammalian caveolin protein, caveolin-1, 2 and 3, of which caveolin-3 is specific to striated muscle (Tang, *et al.* 1996). Myoblast differentiation induces expression of the caveolin-3 gene (Galbiati, *et al.* 2000). Caveolin-3 is the main structural protein for caveolae in skeletal muscle (Galbiati, *et al.* 2000). Caveolin-3 is shown in myotubes to localize at the sarcolemma where it forms a complex with dystrophin (Galbiati, *et al.* 2000; Galbiati, *et al.* 1999). Many signaling molecules co-localize with caveolin-3, including PKC $\alpha$ , Src, MEK, ERK, H-Ras, G-

proteins, and e-Nos (Galbiati, *et al.* 2000). Caveolin-3 binds to these molecules in their inactive form (Pol, *et al.* 1998). This association may play an important role in mechanotransduction via caveolae.

The ERK cascade consists of three sequentially activated kinases: Raf-1 or B-Raf that phosphorylates MEK which phosphorylates ERK1/2. In turn, Raf-1 is activated by Ras, and both can be activated by PKC $\alpha$ . The most characterized results of the ERK MAPK cascade are regulation of cellular proliferation and control of the cell cycle (Sweatt, 2001). ERK has been shown to be quickly and strongly upregulated following stretch (Sadoshima and Izumo, 1993; MacKenna, *et al.* 1998). The association of the entire MAPK cascade with caveolae suggests that caveolae play an important role in transferring mechanical signaling from the cell surface to an ERK2 response.

The associations of caveolae with these signaling molecules in their inactive state as well as the physical evidence that caveolae undergo deformation following stretch suggests that caveolae play an important role in transferring mechanical signal of stretch to the cell interior.

### 1.3 Hypothesis

The work outlined above suggests a mechanism by which mechanical deformations may lead to activation of biochemical signaling. The importance of mechanical signaling to muscle's normal maintenance and function has been extensively studied. There is, however, no clear explanation for the transfer of the external mechanical signal to the resulting biochemical signal. Caveolae associate with and

inhibit signaling molecules involved in muscle growth and hypertrophy. Caveolae also are deformed following stretch, a change in conformation that may rearrange the carefully organized caveolin oligomeric structure. This disruption may eliminate the inhibitory influence of the caveolin scaffolding domain on signaling molecules, resulting in the dis-inhibition of those signaling molecules. We hypothesize that stretch-induced activation of ERK2 is mediated by caveolin-3.

#### 1.4 Experimental Design

Primary neonatal myoblasts were chosen because they have proven to be more myogenic in nature than established lines (Silberstein, *et al.* 1986). A concern when using whole muscle is that being a whole muscle, there are other forces present which are capable of altering, for example, the response of a signaling cascade to an applied stretch. Using primary myoblasts allows for a very controlled environment and more believability in recorded results.

Following the choice of primary myoblasts over whole muscle, a stretch protocol had to be chosen. Uniaxial stretch was chosen because skeletal muscle cells grow and fuse in a uniaxial direction both in culture and in whole muscle. ERK2 was chosen as the illustrative signaling molecule due to the large amount of data previously gathered on it and the relative ease with which it can be measured. For the actual protocol, three repeats of each experiment were performed to acquire enough data to be not only believable but also significantly measurable. This helped also to keep sample number high even if membrane failure occurred before or during the stretch experiment.

The widely used protocol of cholesterol chelation via methyl-beta-cyclodextrin and the protocol for caveolae solidification via temperature control were used to alter caveolae deformability following stretch. The cholesterol chelation experiments were designed based off preliminary work by another member of the lab. A series of concentrations were used at first ranging from 0 to .75% cyclodextrin, and the final concentrations that were chosen were done so based off of cell viability following incubation in cyclodextrin.

The temperature block experiments, which has been used in the past to alter caveolin shuttling to and from the cell surface, was used to attempt to make the caveolae more rigid, the opposite of the effect of cholesterol chelation on the caveolae. However, these protocols are systemic in nature.

siRNA knockdown which specifically blocks caveolin-3 expression was chosen for its short preparation time and the specificity of the experiment. siRNA was used to test the specific involvement of caveolin-3. It was hoped that a complete picture of the role of the caveolae structure and caveolin-3 in ERK2 activation would provide support for the hypothesis.

There was some concern that transfecting the primary myotubes with siRNA might alter the cells' natural responses to cyclic stretch. A series of controls were selected to not only give a visual account of what was occurring in the transfected cells (non-silencing and immunostaining transfections), but also to show numerically any differences between the non-transfected and transfected populations (fusion index, myotube diameter, and myosin content.)

## CHAPTER 2

### METHODS AND MATERIALS

#### 2.1 Isolation and Growth of Neonatal Mouse Myoblasts

##### *2.1.1 Isolation of Neonatal Mouse Myoblasts*

Myoblasts were isolated by enzymatic digestion of hind limb musculature (Rando & Blau, 1994). Two-five day old CFW mouse pups (Swiss-Webster, Charles River Labs) were sacrificed by carbon dioxide asphyxiation, decapitated, and immersed in 70% ethanol. Hind limbs were removed from 3-4 pups at a time and kept on ice. The muscle tissue was dissected from the bone and skin, and minced with razor blades in 0.5 mL of dissociation solution (PBS containing 10 mM CaCl<sub>2</sub>, 1.5 U/ml collagenase, 2.4 U/ml dispase). The minced muscle was removed to a 15 mL centrifuge tube, and the dish was washed with another 0.5 mL of dissociation solution. The tissue slurry was incubated for 30 min at 37°C. The slurry was filtered through a 100 µm mesh strainer into a 50 mL centrifuge tube, the strainer was rinsed with an additional 5 mL of growth media (Ham's F10 nutrient solution (F10) supplemented with 20% FBS, 2.5 ng/ml bFGF, 100 IU/ml penicillin and 100 µg/ml streptomycin), and the cells pelleted for 5 min at 350x gravity. The cell pellet was resuspended in 12 ml of F10. Cells were plated on collagen-coated dishes and identified as passage 0. Myoblasts were purified from fibroblasts and adipocytes through 10-12 successive passages by selective trypsinization and differential

adhesion (Rando & Blau, 1994). In the following experiments, no passage older than P19 was used due to observed changes in morphology at that time.

### *2.1.2 Myogenic Testing*

Myogenicity was evaluated by desmin, which is only expressed in myogenic cells. Cells were plated on a 6-well dish and allowed to proliferate. The cells were rinsed twice with phosphate buffered saline (PBS) and fixed for 5 min in 4% paraformaldehyde in PBS. The wells were then rinsed with PBS and permeabilized for 5 min in 1% Triton X-100 in PBS. The wells were rinsed once more in PBS and blocked in 5% BSA in PBS for 1 hour. Cells were incubated with 1:200 anti-desmin (Vector) for 1 hour. All wells were rinsed 3 times with PBS for 15 min, followed by alkaline phosphatase conjugated anti-mouse secondary antibody (SCBT, 1:100). The wells were rinsed 3 more times with PBS for 15 min and then rinsed with AP buffer (water with 124 mM Tris, 128 mM NaCl, and 6 mM MgCl<sub>2</sub>) for 5 min. The cells were colored with a nitro blue tetrazolium /bromochloroindolyl phosphate solution (NBT/BCIP) until color developed. The cells were rinsed with water and covered with glycerol.

Cells were imaged using phase contrast and conventional illumination. For each picture the cells were counted and the percentage of desmin-positive cells calculated. Only populations exceeding 90% myogenic cells were used in further experiments.

## 2.2 TEM Pictures

C57 primary cells or *mdx* cells were seeded onto matrigel-coated cassettes as previously described. Following myoblast fusion into myotubes, cells were rinsed and fixed for 1 hour in 1.6% paraformaldehyde and 3% glutaraldehyde in 100 mM sodium cacodylate buffer (pH 7.3) at 4°C. They were then washed in 3.5% sucrose in cacodylate buffer and post-fixed in 1% Palade's OsO<sub>4</sub> for 1 hour. Membranes were stained en bloc with uranyl acetate, dehydrated and fixed in epoxy. Sections were cut at 90 nm and viewed by transmission electron microscopy and photographed.

## 2.3 Cell Maintenance and Membrane Seeding

Cells were passed every other day. Cells to be passed were washed twice with PBS and incubated for two minutes with 1.5 mL trypsin. Following trypsin incubation 13.5 ml of growth media was added, and the cells collected in a 50 mL tube. An aliquot of the cells was collected for determination of cell number, and the tube was centrifuged at 100x gravity for 10 minutes. After centrifugation the cell pellet was resuspended in F10 media. Cells were seeded at  $5-10 \times 10^3 \text{ cm}^{-2}$  on collagen coated culture dishes or  $10^4 \text{ cells/cm}^2$  on matrigel coated stretcher cassettes.

## 2.4 Stretch Experiment Prep.

### 2.4.1 Stretch Apparatus

The cassettes consist of a silastic sheet mounted in clamshell shaped clamps to form wells (Figure 2.1). After the cassette was built, a u-clamp was attached to the top of the cassette and the cassette stretched to 1.9 inches. The cassettes were autoclaved and coated with 0.2 mg/ml growth factor reduced matrigel (Becton Dickinson). The matrigel was allowed to gel overnight at 37°C, after which the membranes were washed twice with PBS.

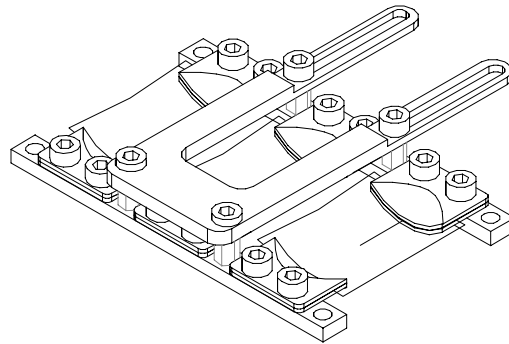


Figure 2.1 – Stretcher Cassette

#### 2.4.2 CFW Growth on Membranes

Cells were allowed to proliferate in growth media up to two days after passage. At roughly 70% confluence, the membranes were stretched to 2.2 inches (25% of seeding length) (Burkholder 2003) to promote unidirectional fusion of the myotubes as seen in Figure 2.3. Stretches were performed using a custom, stepper motor driven device controlled by Labview software (Figure 2.2). Following the stretch, media was changed to differentiation media (Dulbecco's Modified Eagles Media (DMEM) plus 2% horse serum and antibiotics) to promote differentiation of the cells. Cells were allowed to differentiate into myotubes for 2-3 days without media change.

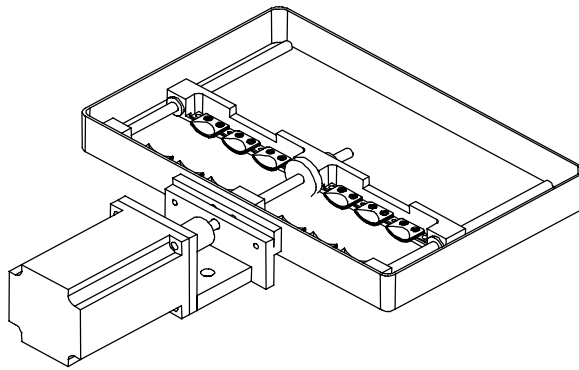


Figure 2.2 – Cassette Stretcher

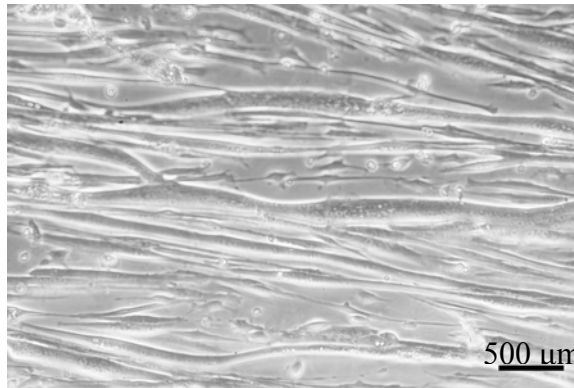


Figure 2.3 – Image of aligned and fused myotubes grown on a well of a cassette

## 2.5 Stretch Experiments

### 2.5.1 Stretch Protocol

Cultures were pre-incubated in CMG (PBS with 0.01%  $MgCl_2$ , 0.015%  $CaCl_2$ , and 0.07% glucose) prior to stretch. Membranes were stretched uniaxially at 37°C for 10 minutes at +/- 15% rest length. Following stretch the membranes were washed in ice cold PBS twice and harvested in 100-150  $\mu L$  of non-denaturing lysis buffer (NDL, water with 1% Triton-X 100, 0.05 M tris, 0.25 M NaCl, 0.025 M EDTA, 0.1% protease inhibitors, and 4 $\mu g/ml$   $NaVO_3$ ) was added. Samples were incubated for 30 minutes on ice. The lysates were centrifuged for 5 minutes at 6000x gravity to remove cellular debris. Protein concentration was measured using a Bicinchoninic Acid Protein Assay (BCA). All samples were stored at -20°C prior to assay.

### *2.5.2 Modifications of Caveolae*

To disrupt the caveolae structure, some cultures were incubated for an hour in CMG plus 0.1% or 0.5% methyl-beta-cyclodextrin (M $\beta$ CD) to chelate cholesterol and disrupt caveolae structure. To increase the rigidity of caveolae, some cultures were held at room temperature for the final 15 minutes of the pre-incubation. Stretch of those cultures was also carried out at room temperature. Additional membranes remained static, at either room temperature or 37°C to serve as controls. Following temperature control or cholesterol chelation, cultures were treated with the addition of FGF to assess the viability of the cell population and test for non-specific disruption or saturation of ERK2 signaling. The time course included a 0, 5, 15, 25, and 40 minute time point encompassing both before and after the time course of a normal stretch experiment

## 2.6 Caveolin-3 Knockdown

### *2.6.1 siRNA Protocol*

Three validated siRNA's previously tested for specific caveolin-3 mRNA knockdown were evaluated for knockdown efficacy. RNA oligos were transfected into differentiated myotubes using a commercially available cationic lipid reagent (Oligofectamine, Invitrogen), according to the manufacturer's instructions. Briefly, siRNA was diluted to 18.3  $\mu$ g/ml in serum free DMEM, and oligofectamine was diluted 1:5 in serum free DMEM. These mixtures were centrifuged briefly and incubated at

room temperature for 5 minutes. The diluted lipid reagent was then added 2:9 to the siRNA mixture and incubated a further 15 minutes at room temperature. The cells were rinsed once with serum free DMEM, and bathed in serum free DMEM. Lipid:RNA complexes were applied to the cells, and an equivalent amount of lipid reagent was applied to control cultures. Cultures were incubated with the transfection mixture for 6 hours, rocked every 2 hours, and then supplemented with 125  $\mu$ L per well of DMEM plus 6% Horse serum. Parallel cultures were transfected with fluorescein-tagged non-silencing RNA oligomers (Qiagen) and imaged under epifluorescent illumination to determine transfection efficiency. Cultures were maintained for an additional 2 days, harvested in detergent buffer, and assayed for caveolin-3 expression by Western blot. Pilot experiments indicated that that the three oligomers resulted in equivalent knockdown ( $91.2 \pm 8.9\%$ ,  $91 \pm 5\%$ , and  $86.5 \pm 6.6\%$ ), and the "cav3-1" oligomer (5'-GGACAUUGUGAAGGUAGAUtt-3') was used for all further experiments.

### *2.6.2 Time Course of knockdown*

Transfected cultures were harvested at 6, 12, and 24 hours following transfection to evaluate the time-course of caveolin-3 knockdown following siRNA transfection.

## 2.7 Bicinchoninic Acid Protein Assay

A set of eight standards was made using 160  $\mu\text{L}$  of tris, sodium chloride, and EDTA (TNE) in the first well and 100  $\mu\text{L}$  in the following seven wells. Forty microliters of 10 mg/ml bovine serum albumin (BSA) was added to the first well and the following six wells were consecutively diluted down by adding 100  $\mu\text{L}$  from the previous well. Standards and samples were loaded as duplicates into a spectrophotometer plate at a volume of 10  $\mu\text{L}$  per well. Using a kit purchased from Pierce, a dyeing solution of 10 ml of protein assay reagent A (sodium carbonate, sodium bicarbonate, BCA detection reagent, and sodium tartrate in 0.1 N sodium hydroxide) per 200  $\mu\text{L}$  of protein assay reagent B (4% cupric sulfate) was made, and 200  $\mu\text{L}$  of the solution was added to each well. The plate was incubated at 37°C for thirty minutes. The plate was read at 562 nm in the spectrophotometer using KCJr software.

## 2.8 Protein Analysis

All protein samples were separated by SDS-PAGE using 7.5, 9, 10, or 12% acrylamide gels. For Western blotting, proteins were transferred for one hour at 1.5 mA per  $\text{cm}^2$  onto a nitrocellulose membrane using a semi-dry transfer system. Following transfer, the membranes were blocked with 1% BSA, hybridized with primary antibodies against ERK2 (Transduction Laboratories), phosphorylated ERK (Cell Signaling), or caveolin-3 (BD). Membranes were incubated for one hour in a blocking solution of 2% BSA in TTBS (water with NaCl, tris-base, tris-HCL, and Tween 20) at room temperature

or overnight at 4°C followed incubation in a primary antibody, three 15 minute rinses in TTBS, incubation with an HRP conjugated secondary antibody (1:20,000), and three more 15-minute rinses in TTBS. Membranes were incubated with ECL (Amersham) for five minutes and exposed to Kodak film. Membranes probed for phospho-specific antibodies were subsequently stripped and re-probed with non-phospho specific antibodies. Films were digitized on a scanner and quantitated using Matlab. ERK2 phosphorylation was determined by normalizing phospho-specific integrated optical density (IOD) to the non-phospho specific IOD. Each sample from a particular film was then normalized to the mean IOD ratio for the control samples from that film.

For assay of myosin content, gels were fixed (50% MeOH, 10% HOAc), and stained with 0.025% Coomassie blue. Gels were extensively destained, scanned, and relative myosin content determined by IOD.

## 2.9 Cell morphology

Fusion index and myotube diameter were measured to evaluate any effect on myotube viability or morphology. Briefly, fusion index was taken by fixing the membranes in 0.4% paraformaldehyde, rinsing in PBS, adding a couple of drops of hematoxylin, acid alcohol, and saturated lithium carbonate, and rinsing again in water. Pictures were taken at 20X magnification. Myotube diameter was measured using Scion Image software.

## 2.10 Immunostaining of Membranes

Caveolin-3 expression following knockdown was also evaluated by immunocytochemistry. Membranes were rinsed with PBS, and fixed with 50% methanol in PBS for 5 minutes. The membranes were rinsed twice and blocked in 5% BSA in PBS for one hour. Cultures were incubated with caveolin-3 antibody (1:100 Santa Cruz) for 30 minutes, rinsed, and incubated with fluorescein-tagged secondary antibody (1:100). The membranes were rinsed twice more in PBS for 5 minutes each and covered in glycerol. Pictures were taken at 20X magnification under epifluorescent illumination.

## 2.11 Statistical Analysis

Results were analyzed by one- or two-way ANOVA using Statview 5.01 (SAS). Fisher's PLSD correction was applied to post-hoc T-tests to evaluate specific differences between treatments. The significance threshold was set to  $p < 0.05$ , and all data are reported as mean  $\pm$  standard deviation.

## CHAPTER 3

### RESULTS

#### 3.1 Myogenic Testing

Desmin immunostaining was used to identify myogenic cells (Figure 3.1). Of the 1398 cells counted in 16 fields,  $99 \pm 1\%$  were desmin positive ( $n = 16$  fields).

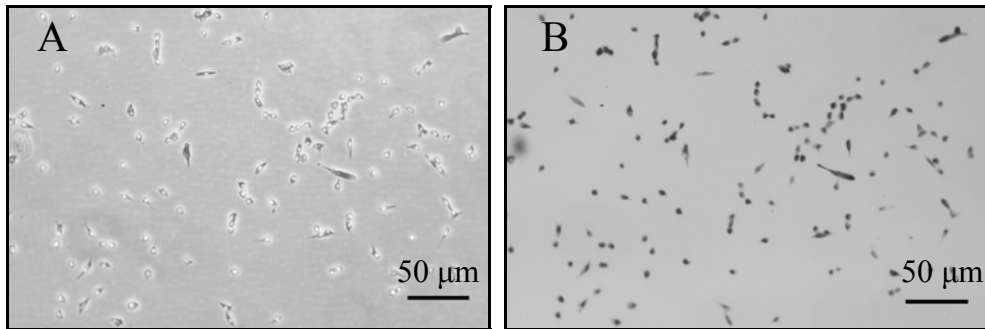


Figure 3.1 – Desmin stained myoblasts in conventional (A) and phase-contrast (B) illumination.

#### 3.2 Fusion Index

Fusion index was determined from 6 visual fields randomly selected from culture wells. Of the 1197 nuclei observed, 90.6% were in multinucleated myotubes. This compares well with the expected range of 70-90% (Rando & Blau, 1994). Individual myotubes contained  $181 \pm 70$  nuclei, reflecting exceptional developmental progression.

### 3.3 Caveolae Morphology

Caveolae morphology in the fused myotubes used in these experiments was evaluated by TEM. Images of stretched myotubes revealed what appeared to be caveolae with a flattened-out morphology, which were not seen in unstretched myotubes (Figure 3.2). TEM images were not quantified in any way and were only used as illustrative evidence.

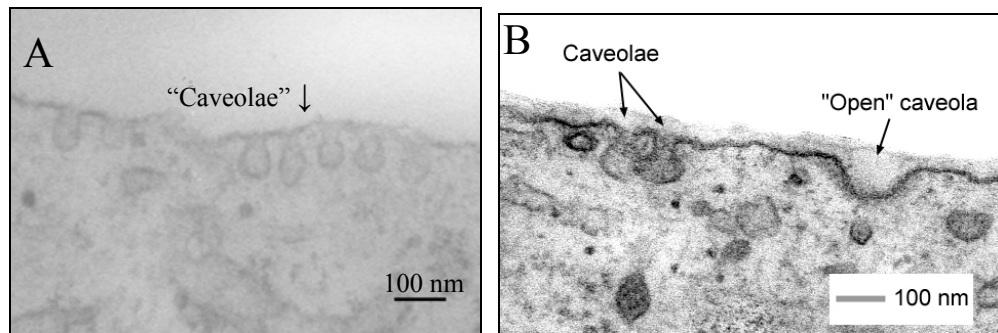


Figure 3.2 – Caveolae-sized structures in unstretched cultures always displayed the classical flask-shaped morphology in *mdx* myotubes (A). Stretched myotubes also displayed putatively pit- or dome-shaped invaginations consistent with opening of caveolae in C57 myotubes (B).

### 3.4 Optimization of the Stretch Protocol

A preliminary series of stretches were used to identify the stretch velocity and amplitude conditions to optimize the detection of ERK2 phosphorylation by stretch. Varying the amplitude and velocity of the stretches (Figure 3.3) revealed that ERK2 activation was affected in a viscoelastic manner. For the varying velocities, a velocity of 20%/second with a 10% amplitude and 40%/second with an amplitude of 15% showed a

significant difference in ERK2 activation of  $p < 0.01$  ( $\dagger$ ). Varying the amplitudes showed a significant increase in ERK2 activation of  $p < 0.01$  (\*) for the 15%, 20% and 30% amplitudes at 20%/second.

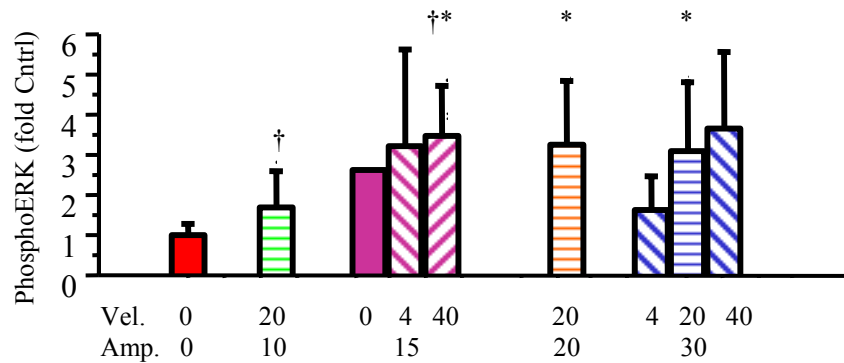


Figure 3.3 –Stretch induced ERK2 phosphorylation depends on both amplitude and velocity. ( $\dagger = p < 0.01$  for velocity,  $* = p < 0.01$  for amplitude, Mean $\pm$ S.D.)

### 3.5 Treatment with Methyl-Beta-Cyclodextrin (M $\beta$ CD)

#### 3.5.1 Stretch Experiments with Methyl-Beta-Cyclodextrin (M $\beta$ CD)

Caveolae are rich in cholesterol, and caveolae morphology can be disrupted by cholesterol sequestration (Li, *et al.* 1996; Smart and Anderson, 2002). Sequestration of cholesterol by 0.1% M $\beta$ CD increased ERK2 phosphorylation in unstretched cultures from  $1.00 \pm .96$  to  $2.8 \pm 2.1$  ( $p < 0.01$ ) and from  $2.0 \pm 1.5$  to  $5.0 \pm 3.0$  in stretched cultures. No statistically resolvable change was found following incubation with 0.5% M $\beta$ CD (Figure 3.4). The lack of significance with the 0.5% M $\beta$ CD pre-incubation may suggest that cell death was occurring at this concentration of M $\beta$ CD or perhaps due to inefficient chelation of cholesterol out of the cells.

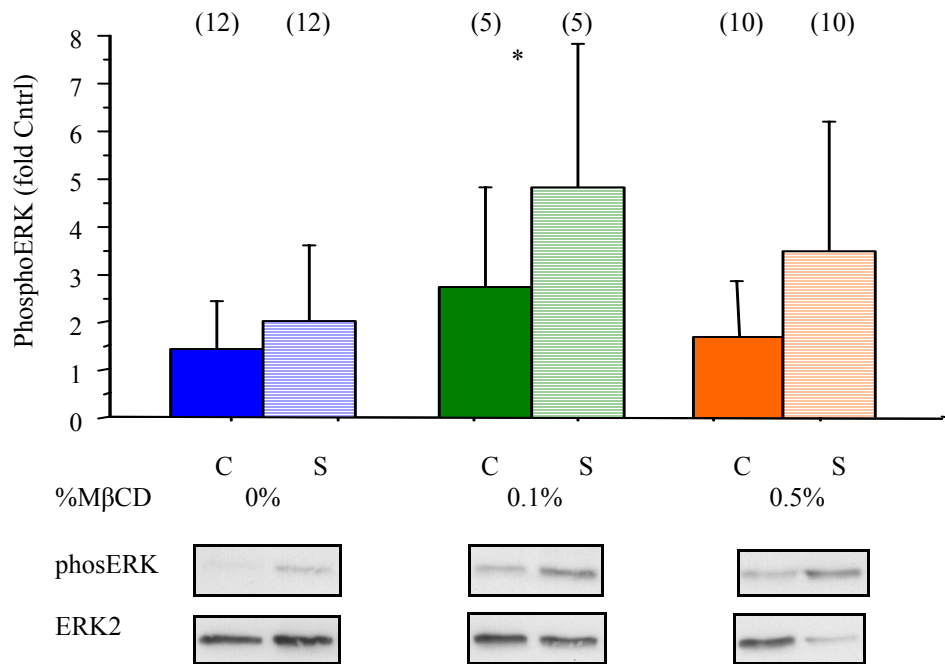


Figure 3. 4 - ERK2 phosphorylation in response to stretch following 1hr pre-incubation with MβCD (\*= $p < 0.01$  for pre-incubation media, Mean $\pm$ S.D.). (parenthetical numbers provide sample number)

### 3.5.2 FGF Experiments with MβCD

A possibility with the MβCD pre-incubation was the saturation of the ERK2 signaling response following chelation of cholesterol. To determine whether this was the case, 0.1% MβCD-treated cells were treated with FGF and harvested at 0, 5, 15, 25, and 40 minutes time points. Static cells treated with 0.1% MβCD responded to bFGF treatment similar to untreated controls (Figure 3.5), indicating that CD treatment does not generally inhibit or alter activation of ERK.

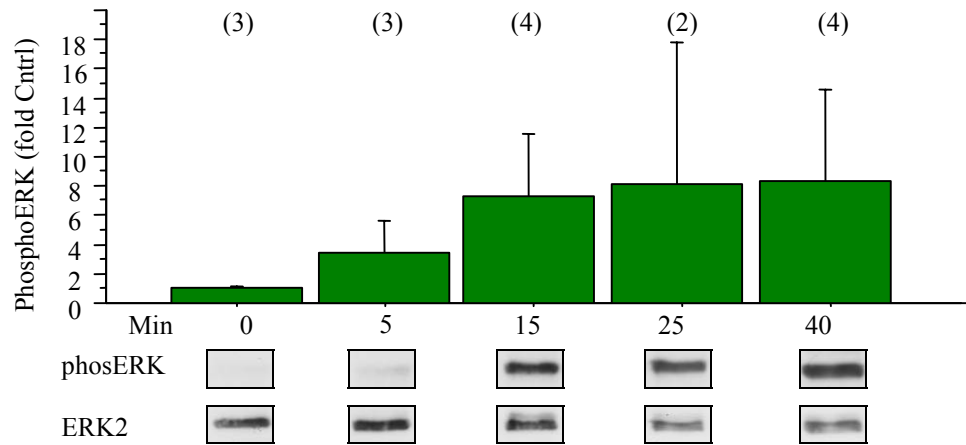


Figure 3. 5 – Static cells treated with 0.1% MβCD over time. (parentetical numbers provide sample number)

### 3.6 siRNA Knockdown

#### 3.6.1 Non-silencing Membrane Transfections

Membranes were transfected with fluorescein-tagged, non-silencing RNA oligomers to evaluate transfection efficiency. Control wells subjected to oligofectamine without the siRNA oligo showed no fluorescence, while 86% of transfected myotubes contained the fluorescent oligomer (Figure 3.6).

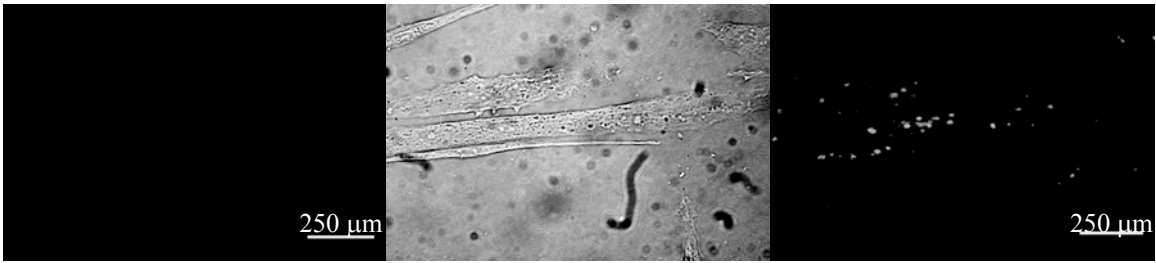


Figure 3. 6 – Transfection with fluorescein-tagged RNA oligos (C) revealed efficient uptake of RNA. Untreated control (A) and light microscope matching “(C)” (B) for comparison.

### 3.6.2 Evaluation of Cav3 siRNA Knockdown

Three validated caveolin-3 siRNA oligomers were evaluated for their relative ability to knockdown caveolin-3 (Figure 3.7). Transfection resulted in significant knockdown compared to the non-transfected controls ( $p < 0.001$ ). Knockdown recorded was  $91.0 \pm 9.0\%$  for cav3-1,  $91.0 \pm 5.0\%$  for cav3-2, and  $87.0 \pm 7.0\%$  for cav3-3.

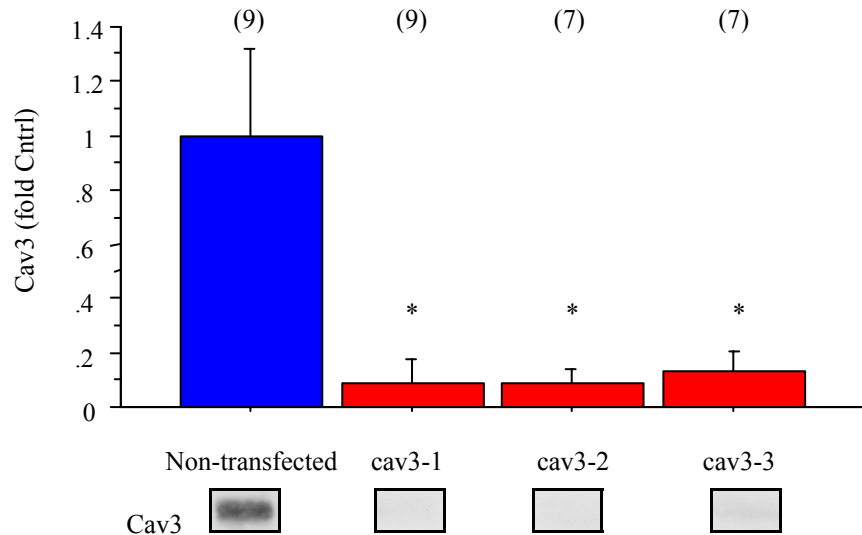


Figure 3. 7 – Static transfection with all three siRNA results in knockdown of caveolin-3 ( $*=p < 0.001$ , Mean $\pm$ S.D.)( parenthetical numbers provide sample number)

Membranes were immunostained with anti-cav3 to assess the presence of caveolae at the membrane surface. The intensity of labeling in transfected cultures was dramatically reduced relative to untreated controls (Figure 3.8). Fluorescence in untreated cultures was strongly associated with the cell membrane, but what fluorescence was apparent in transfected cultures was uniformly distributed within the cytoplasm.

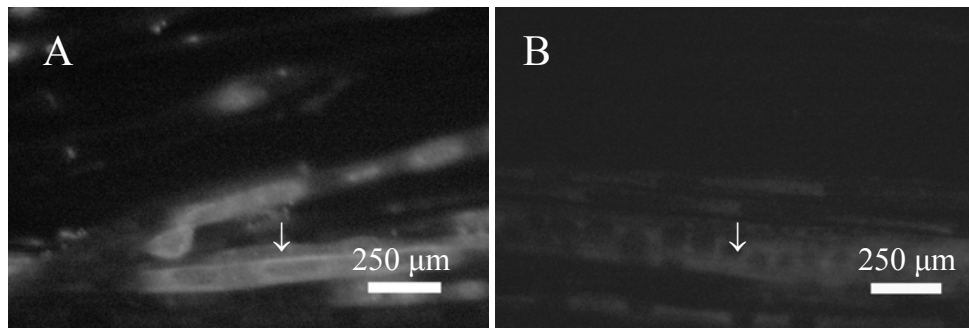


Figure 3. 8 – Immunostaining of a non-transfected (A) and a cav3-1 transfected (B) membrane. In (A) the ↓ refers to the highly localized and membrane-associated caveolin-3. In (B) the ↓ refers to the low fluorescein and distributed caveolin-3.

Phosphorylation of ERK2 was also measured in the static samples for each siRNA to evaluate potential for general disruption of signaling (Figure 3.9). No significant differences were measured in phosphorylated ERK2. Cav3-1 was used for all the following siRNA experiments.

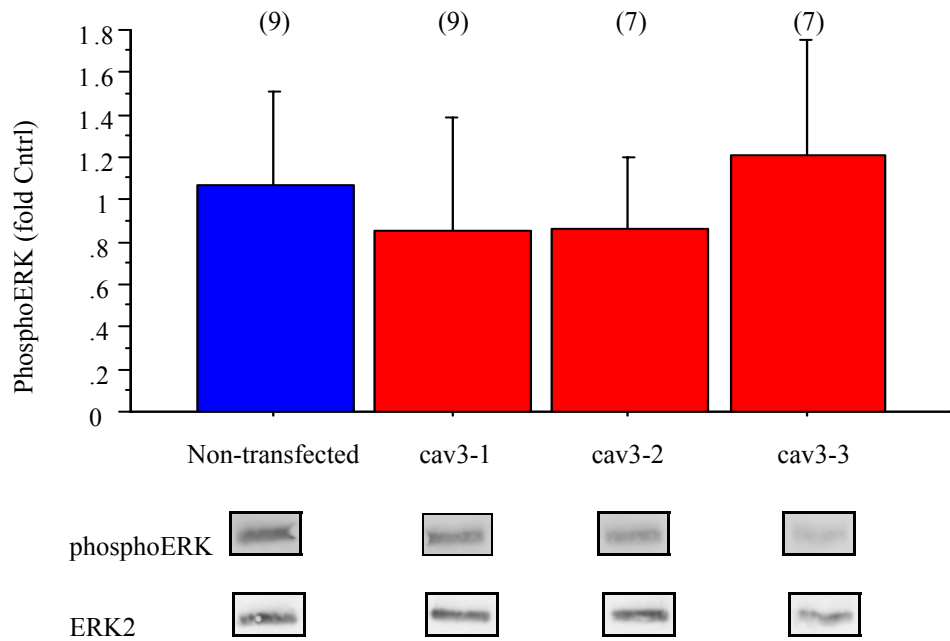


Figure 3. 9 – Alterations in ERK2 activation following siRNA knockdown with all 3 caveolin-3 siRNA's . (parentetical numbers provide sample number)

### 3.6.3 Time Course Study on siRNA Transfected Samples

Cultures were transfected with Cav3-1 siRNA, harvested after 6, 12, and 24 hours, and assayed for caveolin-3 expression. Cav3 expression was significantly reduced ( $p < 0.001$ ) at all time points (Figure 3.10), although differences among time points were not statistically resolvable.

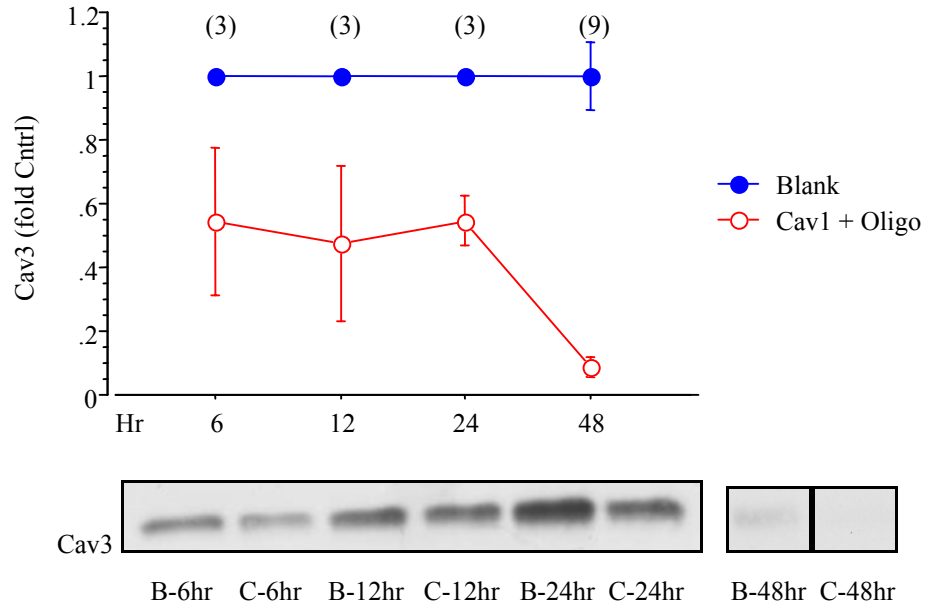


Figure 3. 10 -Time course of Cav-3 knockdown ( $p < 0.0001$  for transfected wells vs. non-transfected,  $MEAN \pm S.E.$ ) (parenthetical numbers provide sample number)

### 3.6.4 Condition of Transfected Myotubes

Transfection did not alter the resting culture conditions of the myotubes.

Transfected myotubes measured at  $232 \pm 42$  fused nuclei per myotube while mononucleated cells measured at  $25 \pm 16$  cells per field counted ( $n = 6$ ). This yields a fusion index of 90%, which is not different from the 91% found in untreated myotubes ( $n = 6$ ). Average myonuclear content of transfected myotubes was  $136 \pm 58\%$  of controls, but this difference is not statistically resolvable.

Myosin content did not differ statistically between the non-transfected and the transfected membranes. Myosin content was  $1.0 \pm 0.5$  for non-transfected controls and  $0.8 \pm 0.5$  for transfected wells ( $n = 40$  wells).

Myotube diameter was measured to determine whether transfection altered fusion rate or cell viability (n = 16). On average, non-transfected myotubes had a diameter of  $20.7 \pm 6.6 \mu\text{m}$ , and transfected myotubes had a diameter of  $21.1 \pm 2.6 \mu\text{m}$ . No significant changes were seen in any of the samples measured.

### 3.6.7 Stretch After Caveolin-3 Knockdown

Myotubes grown on stretch cassettes and transfected with Cav3 siRNA displayed slightly less effective caveolin-3 knockdown of  $50 \pm 26\%$  at the protein level in the unstretched cultures and  $41 \pm 25\%$  in those subjected to knockdown and stretch ( $p < 0.001$ , Figure 3.11).

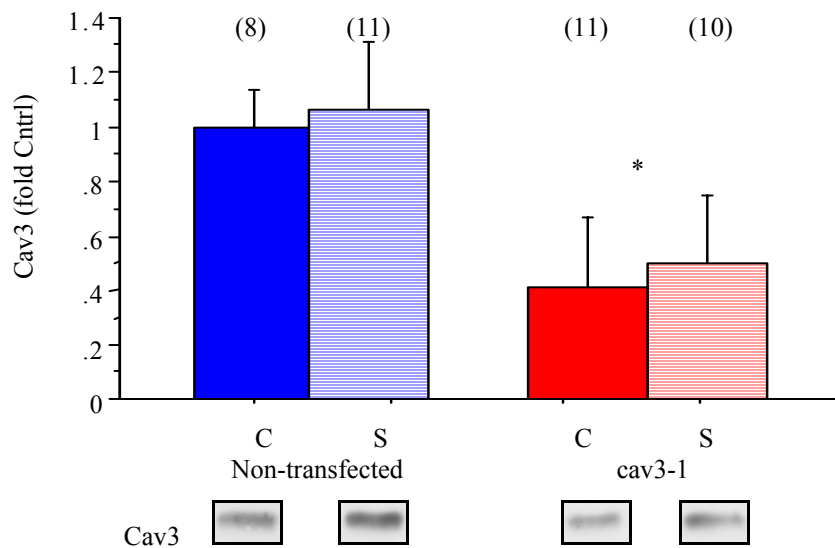


Figure 3. 11– Knockdown of caveolin-3 following transfection with cav3-1 in stretched and unstretched myotubes (\*= $p < 0.001$  for pre-incubation, Mean $\pm$ S.D.)(parenthetical numbers provide sample number).

Despite the less effective knockdown, phosphorylation of ERK2 was significantly different in transfected vs. non-transfected samples ( $p < 0.05$ , Figure 3.12). There was no significant stretch response in the transfected *cav3-1* samples.

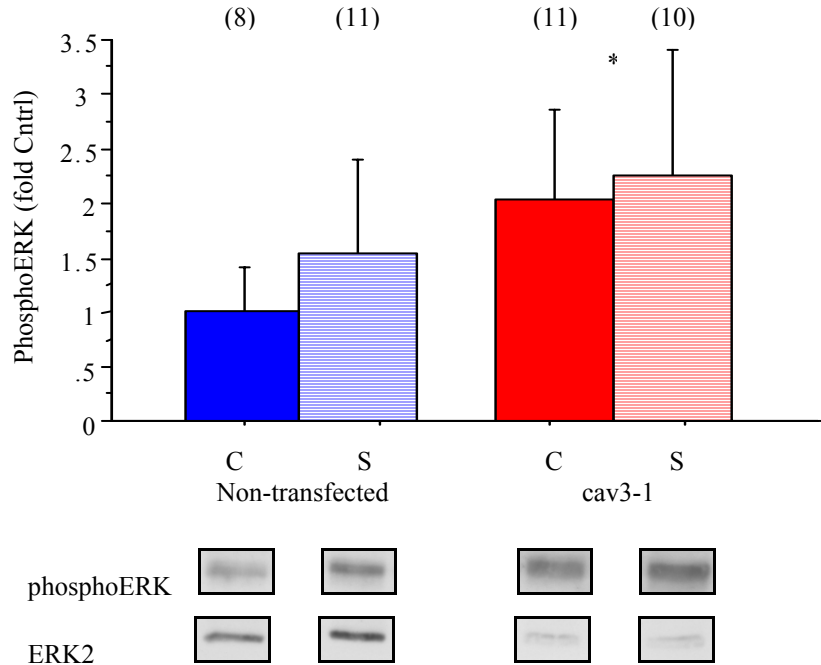


Figure 3. 12– Phosphorylated ERK2 compared in transfected vs. non-transfected cells (\*= $p < 0.05$  for pre-incubation, Mean $\pm$ S.D.)( parenthetical numbers provide sample number).

### 3.7 Stretch Experiments at 22°C

To minimize the deformation of caveolae by stretch, cultures were held at 22°C during stretch. This treatment was intended to induce a liquid to gel phase transition in the caveolae, increasing their rigidity and resistance to deformation and blocking stretch activation of ERK2. Interestingly, the reduction in temperature

significantly reduced the caveolin-3 recovered from cultures (Figure 3.13). Caveolin-3 dropped to  $11 \pm 9\%$  in the  $22^\circ\text{C}$  non-transfected, unstretched controls and  $20 \pm 11\%$  in the  $22^\circ\text{C}$  non-transfected, stretched cultures. Differences between control and stretch samples were not resolvable.

Myosin content dropped from  $90 \pm 40\%$  in the  $37^\circ\text{C}$  samples to  $60 \pm 30\%$  in the  $22^\circ\text{C}$  samples ( $p < 0.01$ ), suggesting that the temperature dependent differences likely reflect the selective loss of Cav-3 containing myotubes over Cav-1 expressing myoblasts.

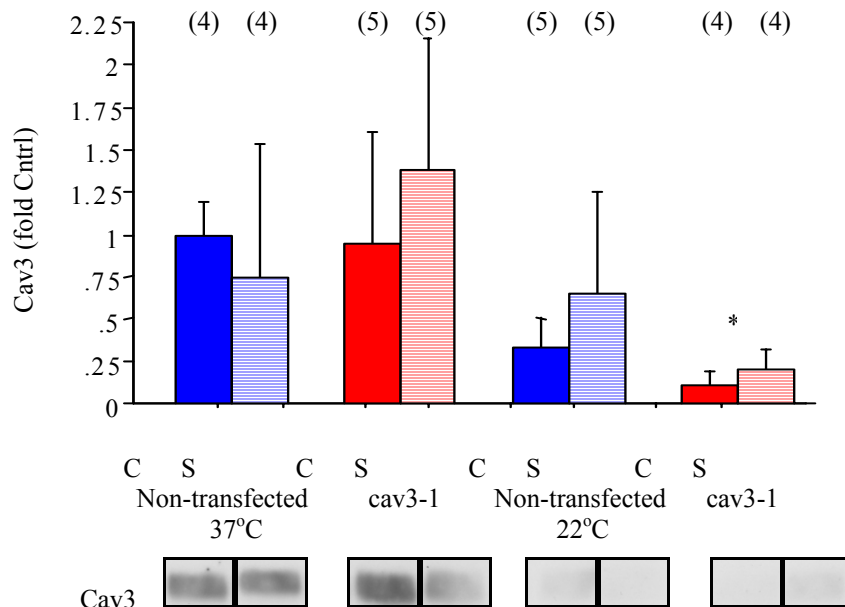


Figure 3. 13– Caveolin-3 expression in  $37^\circ\text{C}$  and  $22^\circ\text{C}$  samples with and without previous transfection (\*= $p < 0.005$  for pre-incubation, MEAN $\pm$ S.D.)( parenthetical numbers provide sample number)

Phosphorylation of ERK2 was significantly different between the  $37^\circ\text{C}$  and  $22^\circ\text{C}$  samples ( $p < 0.02$ ); the  $22^\circ\text{C}$  samples had an increase of activation of  $230 \pm 130\%$  in the unstretched controls and  $180 \pm 80\%$  in the stretched group. ERK2 phosphorylation was

also significantly different between the 37°C non-transfected samples and the cav3-1 transfected membranes (Figure 3.14,  $p < 0.002$ ), increasing in the transfected membranes  $410 \pm 350\%$  in the controls and  $170 \pm 120\%$  in the stretches. The 22°C non-transfected samples were also significantly different from the 22°C cav-3 transfected membranes ( $p < 0.05$ ).

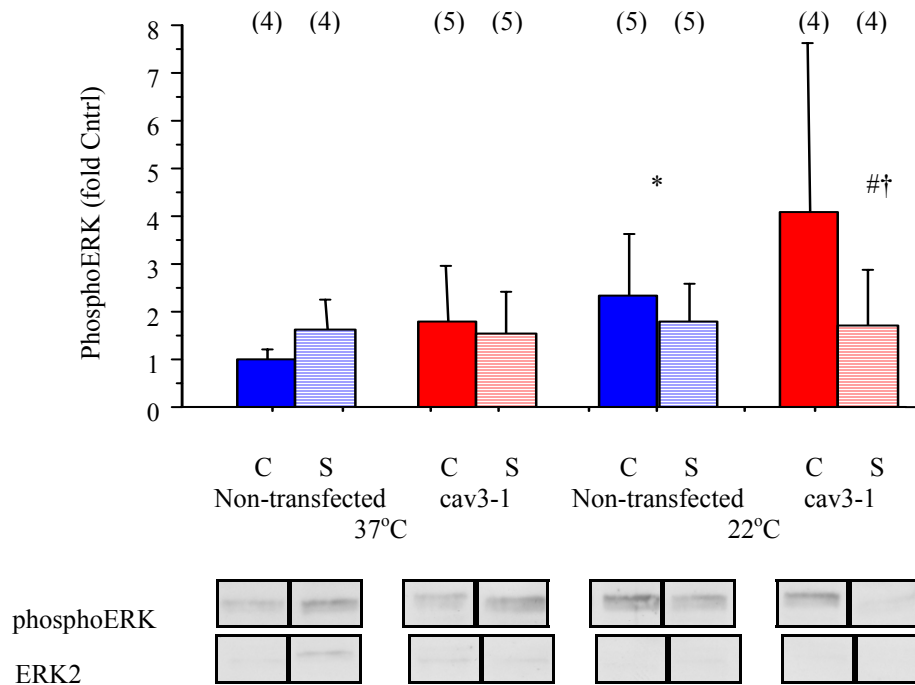


Figure 3. 14 – PhosphoERK activation in the 37°C vs. 22°C samples (\*= $p < 0.02$ , #= $p < 0.002$ , †= $p < 0.05$  by pre-incubation, MEAN $\pm$ S.D.)( parenthetical numbers provide sample number)

### 3.7.1 FGF Responsivity Experiment

To evaluate whether the reduced temperature generally disrupted intracellular signaling, cultures were held at 22°C, treated with 2.5 ng/ml bFGF and harvested at 0, 5, 15, 25, and 40 minutes. FGF treatment at room temperature increased ERK2 phosphorylation (Figure 3.15,  $p < 0.01$ ) to an extent comparable with cultures at 37°C.

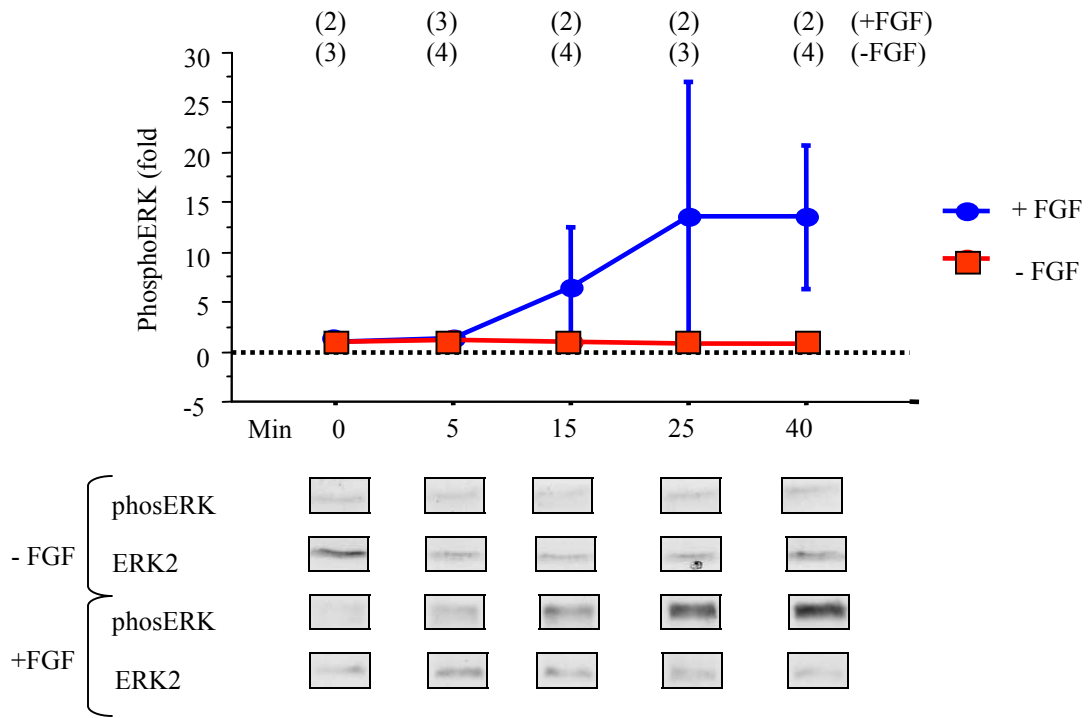


Figure 3.15 - FGF stimulated ERK2 phosphorylation at room temperature (22°C), (parentetical numbers provide sample number)

## CHAPTER 4

### DISCUSSION

We hypothesized that stretch-induced activation of ERK2 is mediated by caveolin-3. From previous data, we know that caveolae unfold during stretch and that caveolin-3 binds to and inhibits several signaling molecules involved in the stretch response (Dulhanti and Franzini-Armstrong, 1975; Galbiati, *et al.* 2000; Pol, *et al.* 1998). We suggest that following stretch, caveolin-3, and thus the signaling molecules it is bound to, is pushed off the caveolae structure causing a conformational change in how it is bound to the signaling molecules. This in turn allows those molecules, such as ERK2, to become activated and carry out their downstream tasks.

Our data shows that caveolin-3 does play an important role in the stretch-induced activation of ERK2. Knockdown of the caveolin-3 protein by 50% results in the loss of the stretch-induced ERK2 activation. Morphological data and myosin content indicate that transfection does not fundamentally alter the cells, supporting the idea that it is the loss of caveolin-3 protein that causes the loss of ERK2 activation.

As explained above, caveolin-3 inhibits ERK2 to maintain a low resting activity (Pol, *et al.* 1998). The loss of the stretch response seen after knockdown may explain why muscular dystrophies have the phenotypes they do. From previous research it is known that LGMD-1C is characterized by a loss of caveolin in the skeletal muscle cells, similar to using siRNA to knock down caveolin-3 expression (Galbiati, *et al.* 2000; Minetti, *et al.* 2002). Muscles of LGMD-1C patients, as a result, undergo myopathic changes and other alterations in the cells' signal transduction machinery such as the t-

tubule system (Galbiati, *et al.* 2000). In the siRNA protocol, transfected cells show an increase in basal levels of ERK2 activation but a loss of the ERK2 stretch-response. Removing caveolin-3 from the cells may distort or completely remove caveolae present at the cell surface. This, in turn, may allow for the signaling molecules normally associated with and inhibited by caveolin-3 to become chronically activated. If deformation of the caveolae structure is necessary for normal activation and deactivation of these signaling cascades, this could explain why patients with LGMD-1C show signs of continual muscle turnover and alterations in the cells' mechanotransduction machinery. Disruption of the caveolae structure would lead to chronic activation of the signaling cascades, as well as, a loss in the cells' ability to control their activation via caveolae deformation. This idea can also be taken and used to explain other disease phenotypes due to chronic activation of any of the other signaling molecules and cascades associated with caveolae.

Other less specific protocols were also used to attempt to connect the importance of normal caveolae deformation following stretch and signaling cascade activation/deactivation. Destabilization of the caveolae structure was attempted via cholesterol chelation using methyl-beta-cyclodextrin. Cholesterol is an important member of the caveolae structure. It interacts with sphingolipids to create the liquid-ordered state present in caveolae (Veiga, *et al.* 2001). The physical effect of cholesterol depletion is dependent on the specific distribution of cholesterol in the cell. Pre-incubation with 0.1% M $\beta$ CD resulted in increased ERK2 activation in both static and stretched cultures. Pre-incubation with 0.5% M $\beta$ CD showed no difference with ERK2 activation in untreated cells that was inconsistent with the 0.1% M $\beta$ CD samples' data. In

the same way that knockdown of caveolin-3 with siRNA led to an increase in the basal levels of ERK2 activation, treatment with M $\beta$ CD may cause the overall increase in ERK2 activation. Chelation of cholesterol may be enough to destabilize the caveolae structure, driving off some of the caveolin-3, and resulting in an increase in the basal level of ERK2 activation. It is not able, however, to destabilize the caveolae structure enough to remove the stretch response. Thus, the 0.1% M $\beta$ CD data is consistent with destabilization of caveolae in the context of the proposed model offering additional data that confirms that normal deformation of caveolae and the resulting alterations in caveolin-3 are necessary for control of the signaling molecules associated with caveolin-3.

It should be noted that using M $\beta$ CD to chelate cholesterol specifically out of caveolae, while a common protocol, is highly sensitive to application (Smart & Anderson, 2002). Without assaying the morphology of caveolae by EM, or the association of caveolin with lipid rafts by gradient fractionation, it is not possible to be certain exactly what the cyclodextrin treatment accomplished. Cells did respond as expected to stimulation with bFGF, though, so it is not likely that the inconsistencies in the data resulted from massive cell death or extensive disruption of intracellular signaling for the 0.1% M $\beta$ CD pre-incubation.

Pre-incubation at room temperature was used to minimize the deformation of caveolae by stretch by inducing a liquid to gel phase transition in the caveolae, increasing their rigidity and resistance to deformation. An increase in basal levels of ERK2 activation was seen in the 22°C samples with a loss of the stretch-response in both non-transfected and transfected samples. Transfected samples were also significantly different than the non-transfected ones at 22°C. This suggests that the caveolae structural

integrity matters for proper inhibition of the ERK2 cascade, and that removal of caveolin-3 will accomplish the same thing as temperature control, increasing the basal level of ERK2 activation and removing the stretch-dependent response.

It was thought that lowering the temperature of the cells and gelling the sphingolipids in the caveolae would minimize caveolae deformation and block ERK2 activation by stabilizing the association between membrane-bound caveolin and ERK2. The overall increase in ERK2 activation in the cold samples, however, suggests that the unique liquid-ordered properties of these rafts are key in the inhibition of the signaling cascades. This could be due to disruption of the striated caveolin coat that covers the entire caveolae surface. Gelling the caveolae may result in local deformation of how caveolin binds to the other structural elements of caveolae, to itself, and even to the signaling molecules associated with it. Deformation of caveolin would then alter the way it binds and inhibits signaling molecule activation allowing for the signaling molecules to bind to other factors and become activated. This suggests that disruption of the natural ordered structure of caveolae is a viable means by which signaling molecules can become exposed in a way that allows for their activation to occur.

Pre-incubation at 22°C had the unexpected result of significantly lowering the amount of caveolin-3 measured in the samples. Myosin levels were compared in these samples, and it was seen that there was a significant drop in myosin in the 22°C samples. This may mean that pre-incubation is resulting in at least the partial death of myotubes leading to the lower levels of caveolin-3 and myosin measured in the temperature control samples. However, the myotubes present still responded as expected to FGF stimulation. This may indicate that even if there is some cell death occurring, it is not enough to alter

the cells still present and their natural stretch-induced responses. This may also indicate only that ERK2 activation is not being saturated in these particular samples even if the natural stretch-response has been altered by the protocol.

Further work needs to be done to verify the data shown in this paper. Following up on the siRNA work, other cascades either associated with ERK2 and caveolae, such as nNOS, PLA2, and a variety of G-proteins, or associated with the general hypertrophic response could be studied to attain a better feel for what was occurring in the knockdown cells.

To improve visually our understanding behind what was occurring in these cells, both transfected and non-transfected, more TEM pictures could be taken so as to be able to actually quantify the caveolae present. Staining in the TEM pictures for caveolin-3 would also be helpful in determining whether or not the structures seen were indeed caveolae. The immunostained samples could also be dually stained with a phosphoERK antibody to visualize whether what is believed to be caveolin-3 truly is the molecule associated with ERK2. To study whether the changes in ERK2 activation were only due to increased disruption of the membranes, a reason perhaps for the increase in caveolae in DMD patients' cells, Fdx assays could also be run.

#### 4.1 Clinical Importance

As suggested in the introduction, caveolae may open when muscles are stretched. In addition to its role in controlling signaling cascades, caveolae may act as sources of excess membrane during stretch protected cells from membrane disruption or injury. In

combination with the association of caveolin-3 with multiple inactive signaling molecules, this implies that caveolae may play an important role in the maintenance of skeletal muscle. If caveolae are truly present to act as a means by which signaling cascades are activated during stretch, then the associated muscle growth with passive bone growth might be a result of constant, though low, activation of signaling cascades due to caveolae deformation and alterations in the caveolin-3 binding to the signaling molecules.

One of the most common means to treat high blood cholesterol is to prescribe some form of statin, which block the synthesis of cholesterol, leading to reductions of circulating cholesterol. Among the major side effects of statins is muscle weakness and pain, and it may be that reducing the body's cholesterol levels mimics the M $\beta$ CD chelation of cholesterol out of the caveolae (Moghadasian, 2002). The disruption of the caveolae structure and the potential loss of caveolae due to the taking of statins may lead to chronic increases in basal activation of ERK2 and, in turn, muscle loss causing pain and weakness.

LGMD-1C, which results in the extreme loss of caveolin-3 from the cell surface, may in turn be an extreme example of the effects of disrupting caveolae structure and caveolin-3 function (Galbiati, *et al.* 2000; Minetti, *et al.* 2002). The resulting phenotype in LGMD-1C patients may be due to the chronic activation of ERK2 and all its downstream targets (Woodman, *et al.* 2002), as well as, the loss of the cells' ability to mediate ERK2 activation via stretch.

Showing that caveolin-3 is important for the ERK2 stretch-induced response is a step in uncovering how caveolin-3 mediates mechanotransduction in skeletal muscle

cells. It may help explain some of the phenotypic effects of muscular dystrophies, and eventually, help find a cure for them.

## REFERENCES

- Aronson, D., Violan, M.A., Dufresne, S.D., Zangen, D., Fielding, R.A., and Goodyear, L. J. (1997). "Exercise Stimulates the Mitogen-activated Protein Kinase Pathway in Human Skeletal Muscle." J. Clin. Invest. **99**: 1251-1257.
- Carson J.A. and Wei, L. (2000). "Integrin Signaling's Potential for Mediating Gene Expression in Hypertrophying Skeletal Muscle." J Appl Physiol. **88**(1):337-43.
- Chen, Y.-W., Nader, G.A., Baar, K.R., Fedele, M.J., Hoffman, E.P., and Esser, K.A. (2002). "Response of Rat Muscle to Acute Resistance Exercise Defined by Transcriptional and Translational Profiling." J Physiol (Lond). **545**: 27-41.
- Dulhanti, A. and Franzini-Armstrong, C. (1975). "The Relative Contributions of the Folds and Caveolae to the Surface Membrane of Frog Skeletal Muscle Fibers at Different Sarcomere Lengths." J Physiol. (London) **250**: 513-539.
- Florini, J.R., E., D.Z., and Coolican, S.A. (1996). "Growth Hormone and the Insulin-Like Growth Factor System in Myogenesis." Endocrine Reviews **17**: 481-517.
- Galbiati F, Volonte D, Engelman JA, Scherer PE, Lisanti MP. (1999). "Targeted Down-Regulation of Caveolin-3 is Sufficient to Inhibit Myotube Formation in Differentiating C2C12 Myoblasts. Transient Activation of p38 Mitogen-Activated Protein Kinase is Required for Induction of Caveolin-3 Expression and Subsequent Myotube Formation." J Biol Chem. **274**(42):30315-21.
- Galbiati, F., Volonte, D., Minetti, C., Bregman, D.B., and Lisanti, M.P. (2000). "Limb-girdle Muscular Dystrophy (LGMD-1C) Mutants of Caveolin-3 Undergo Ubiquitination and Proteasomal Degradation." The Journal of Biological Chemistry **275**: 37702-37711.
- Goldberg, A.L. (1968). "Protein Synthesis During Work-Induced Growth of Skeletal Muscle." Journal of Cell Biology **36**: 653-658.
- Goldspink, G., Williams, P., and Simpson, H. (2002). "Gene Expression in Response to Muscle Stretch." Clin Orthop. **403**: S146-52.
- Hoffman EP, Brown RH Jr, Kunkel LM. (1987). "Dystrophin: the Protein Product of the Duchenne Muscular Dystrophy Locus." Cell. **51**(6):919-28.
- Kumar, A., Chaudhry, I., Reid, M.B., and Boriek, A.M. (2002). "Distinct Signaling Pathways Are Activated in Response to Mechanical Stress Applied Axially and Transversely to Skeletal Muscle Fibers." J. Biol. Chem. **277**: 46493-46503.

- Le, P.U. and Nabi, I.R. (2003). "Distinct Caveolae-Mediated Endocytic Pathways Target the Golgi Apparatus and the Endoplasmic Reticulum." Journal of Cell Science **116**: 10.1242/jcs.00327
- Lexell, J., Taylor, C.C. et al. (1988). "What is the cause of the ageing atrophy? Total number, size and proportion of different fiber types studied in whole vastus lateralis muscle from 15- to 83-year-old men." J Neurol Sci **84**(2-3): 275-94.
- Li, S., Couet, J., and Lisanti, M.P. (1996). "Src Tyrosine Kinases, Gα Subunits, and H-Ras Share a Common Membrane-anchored Scaffolding Protein, Caveolin." The Journal of Biological Chemistry **271**: 29182-19190.
- Loughna, P.T., Mason, P., and Bates, P.C. (1992). "Regulation of Insulin-Like Growth Factor 1 Gene Expression in Skeletal Muscle." Symp Soc Exp Biol. **46**:319-30.
- MacKenna, D.A., Dolfi, F., Vuori, K., Ruoslahti, E. (1998). "Extracellular Signal-regulated Kinase and c-Jun NH2-terminal Kinase Activation by Mechanical Stretch Is Integrin-dependent and Matrix-specific in Rat Cardiac Fibroblasts." J. Clin. Invest. **101**: 301-310.
- Magana MM, Lin SS, Dooley KA, Osborne TF. (1997). "Sterol Regulation of Acetyl Coenzyme A Carboxylase Promoter Requires Two Interdependent Binding Sites for Sterol Regulatory Element Binding Proteins." J Lipid Res. **38**(8):1630-8.
- Maniotis, A. J., Chen, C.S. et al. (1997). "Demonstration of mechanical connections between integrins, cytoskeletal filaments, and nucleoplasm that stabilize nuclear structure." Proc Natl Acad Sci U S A **94**(3): 849-54.
- Mayer, U. (2003). "Minireview: Integrins: Redundant or Important Players in Skeletal Muscle?" J Biol Chem **278**(17): 14587-14509.
- McKoy G, Ashley W, Mander J, Yang SY, Williams N, Russell B, Goldspink G. (1999). "Expression of Insulin Growth Factor-1 Splice Variants and Structural Genes in Rabbit Skeletal Muscle Induced by Stretch and Stimulation." J Physiol. **516** ( Pt 2):583-92.
- McNeil, P.L. and Steinhardt, R.A. (1997). "Minireview: Loss, Restoration, and Maintenance of Plasma Membrane Integrity." The Journal of Cell Biology **137**: 1-4.
- Minetti, C., Bado, M. et al. (2002). "Impairment of caveolae formation and T-system disorganization in human muscular dystrophy with caveolin-3 deficiency." Am J Pathol **160**(1): 265-70.

- Moghadasian, M.H. (2002). "A Safety Look at Currently Available Statins." Expert Opin Drug Saf. **1**(3):269-74.
- Okamoto T, Schlegel A, Scherer PE, Lisanti MP. (1998). "Caveolins, a Family of Scaffolding Proteins for Organizing "Preassembled Signaling Complexes" at the Plasma Membrane." J Biol Chem. **273**(10):5419-22.
- Pol, A., Calvo, M., Enrich, C. (1998). "Isolated Endosomes from Quiescent Rat Liver Contain the Signal Transduction Machinery: Differential Distribution of Activated Raf-1 and Mek in the Endocytic Compartment." FEBS Lett **441**(1): 34-38.
- Powell, C.A., Smiley, B.L., Mills, J., and Vandeburgh, H.H. (2002). " Mechanical Stimulation Improves Tissue-Engineered Human Skeletal Muscle." Am J Physiol Cell Physiol. **283**: C1557-C1565
- Rando TA, Blau HM. (1994). "Primary Mouse Myoblast Purification, Characterization, and Transplantation for Cell-Mediated Gene Therapy." J Cell Biol. **125**(6):1275-87.
- Repetto, S., B., M., Broda, P., Lucania, G., Masetti, E., Sotgia, F., Carbone, I., Pavan, A., Bonilla, E., Cordone, G., Lisanti M.P., and Minetti, C. (1999). "Increased Number of Caveolae and Caveolin-3 Overexpression in Duchenne Muscular Dystrophy." Biochem. Biophys. Res. Commun. **261**: 547-550.
- Rothberg KG, Heuser JE, Donzell WC, Ying YS, Glenney JR, Anderson RG. (1992). "Caveolin, a Protein Component of Caveolae Membrane Coats." Cell. **68**(4):673-82.
- Rybin, V.O., Xu, X. and Steinberg, S.F. (1999). "Activated Protein Kinase C Isoforms Target to Cardiomyocyte Caveolae: Stimulation of Local Protein Phosphorylation." Circ Res **84**(9): 980-8.
- Sadoshima, J. and Izumo, S. (1993). "Mechanical Stretch Rapidly Activates Multiple Signal Transduction Pathways in Cardiac Myocytes: Potential Involvement of an Autocrine/Paracrine Mechanism." Embo J. **12**: 1681-1692.
- Sadoshima J. and Izumo S. (1997). "The Cellular and Molecular Response of Cardiac Myocytes to Mechanical Stress." Annu Rev Physiol. **59**:551-71.
- Silberstein L, Webster SG, Travis M, Blau HM. (1986). "Developmental Progression of Myosin Gene Expression in Cultured Muscle Cells." Cell. **46**(7):1075-81.
- Smart EJ, Anderson RG. (2002). "Alterations in Membrane Cholesterol that Affect Structure and Function of Caveolae." Methods Enzymol. **353**:131-9.

- Sweatt, J.D. (2001). "The Neuronal MAP Kinase Cascade: A Biochemical Signal Integration System Subserving Synaptic Plasticity and Memory." J Neurochem **76**: 1-10.
- Tang Z, Scherer PE, Okamoto T, Song K, Chu C, Kohtz DS, Nishimoto I, Lodish HF, Lisanti MP. (1996). "Molecular Cloning of Caveolin-3, a Novel Member of the Caveolin Gene Family Expressed Predominantly in Muscle." J Biol Chem. **271**(4):2255-61.
- Tatsumi R, Sheehan SM, Iwasaki H, Hattori A, Allen RE. (2001). "Mechanical stretch induces activation of skeletal muscle satellite cells in vitro." Exp Cell Res. 1:107-14.
- Vaghy, P. L., Fang, J. et al. (1998). "Increased Caveolin-3 Levels in mdx Mouse Muscles." FEBS Lett **431**(1): 125-7.
- Veiga, M. P., Arrondo, J.L., Goni, F.M., Alonso, A., and Marsh, D. (2001). "Interaction of Cholesterol with Sphingomyelin in Mixed Membranes Containing Phosphatidylcholine, Studied by Spin-Label ESR and IR Spectroscopies. A Possible Stabilization of Gel-Phase Sphingolipid Domains by Cholesterol." Biochemistry 40(8): 2614-22.
- Williams, P.E. and Goldspink, G. (1976). "The Effect of Denervation and Dystrophy on the Adaptation of Sarcomere Number to the Functional Length of Muscle in Young and Adult Mice." J Anat. **122**:455-465.
- Williamson D, Gallagher P, Harber M, Hollon C, Trappe S. (2003). "Mitogen-activated protein kinase (MAPK) pathway activation: effects of age and acute exercise on human skeletal muscle." J Physiol. 547(Pt 3):977-87.